COMPDYN 2023
9th ECCOMAS Thematic Conference on
Computational Methods in Structural Dynamics and Earthquake Engineering
M. Papadrakakis, M. Fragiadakis (eds.)
Athens, Greece, 12-14 June 2023

# NUMERICAL MODELLING AND STRUT-AND-TIE CONCEPTS FOR SEISMIC DESIGN AND ASSESSMENT OF PRE-CAST TWO-COLUMN BENTS

**L. Carvalho[1], M. Pimentel[1], P. Delgado[2,1], A. Arêde[1], N. Vila Pouca[1], and J. R. Pinto[3]**

[1] CONSTRUCT, Faculty of Engineering, University of Porto
R. Dr. Roberto Frias, s/n 4200-465, Porto, Portugal
lucasc@fe.up.pt, mjsp@fe.up.pt, aarede@fe.up.pt, nelsonvp@fe.up.pt

[2] proMetheus, Instituto Politécnico de Viana do Castelo
R. Escola Industrial e Comercial de Nun´Álvares, 4900-347, Viana do Castelo, Portugal
pdelgado@estg.ipvc.pt

[3] Mota-Engil, Engenharia e Construção S.A., Porto, Portugal
Rua do Rego Lameiro, nº38 4300-454, Porto, Portugal
jose.r.pinto@mota-engil.pt

## Abstract

*Precast structures are more common in zones not affected by earthquakes or affected by low - to moderate-intensity earthquakes; the application of precast structures in zones of higher seismic intensity is unusual due to the seismic performance uncertainty of these structures. Concerning precast bridges, special attention needs to be paid on the column to cap-beam connections, as well as the methods to anchor the column longitudinal bars into the cap beam or foundation. The constructability of these joints often becomes unworkable due to the high reinforcement concentration that current standards require. Moreover, some design rules are rather unclear and the link to the flow of forces in the joint is sometimes lost. In this paper, to ensure a clear understanding of the forces flow, strut-and-tie concepts were applied to design a column-to-cap-beam joint region of a viaduct located in southern Europe. In addition, different ductility classes were considered. Emphasis was given to nonlinear numerical models developed to validate the strut-and-tie models as well as to evaluate the two ductility scenarios performed. As a modeling strategy, a rotating smeared crack approach was considered; also, constitutive models with fracture energy were considered to simulate the concrete mechanical behavior. Numerical results will be further validated through an experimental campaign planned to assess the structural performance of the designed solution.*

**Keywords:** Bridges, Beam-column joints, Numerical models, Seismic behavior, Pre-cast solutions.

# 1 INTRODUCTION

The search for a more effective process in the construction of bridges that allows increasing the safety of workers and carries out the construction in the shortest possible period, reducing traffic and cost disorders, is an aspect of great importance today and that is being widely applied around the world through the Accelerated Bridge Construction (ABC) method [1]. Among many construction technologies, precast structures are the ones that have the greatest potential to achieve these objectives. However, there are still uncertainties concerning these structures to be applied in zones of medium to high seismicity. An important aspect of the precast bridge substructure design is the connection between the column and the cap beam and the column and the foundation. The design of these regions following existing standards requires a considerable amount of transverse reinforcement inside the joints, leading to reinforcement congestion and constructability problems. Furthermore, the link to the flow of forces in some design rules is not clear and easy to understand.

Based on this, a fully precast column and cap beam solution for railway viaducts will be presented. The seismic intensity considered for design corresponds to a maximum elastic spectral acceleration in the range of 0.7g and 0.75g for Type I and Type II, respectively. Behavior factors ranging from q=3.0 to q=4.5 are being studied to consider different ductility classes. The design was done following the capacity design principles, ensuring energy dissipation on the regions of maximum flexural moments of the columns, avoiding brittle failure modes, and ensuring the integrity of the cap beam supporting the deck. Strut-and-tie models were developed aiming the cap beam design, in view to better understand the force transfer mechanism.

A numerical investigation resorting to three-dimensional nonlinear finite element analyses was done to assess the redistribution of forces, confirm the failure mode, and quantify the ductility/energy dissipation capacity of the designed solution.

# 2 CASE STUDY

## 2.1 General

A double-track railway viaduct with 6 spans of 22m+4x30m+22m, see Figure 1, provides the case study for the solution developed. The continuous deck is bearing supported on 5 intermediate cap beams with two columns each. As shown in Figure 2, the columns are 10m high between the top of the foundation and the base of the cap beam. The deck is constituted by 4 precast longitudinal U-beams in each span. It was considered that the support devices on the cap beam do not transmit longitudinal forces. Thus, the substructure system is in charge of seismic action resistance in the transverse direction, being the transverse forces from the deck transferred through a corbel placed at the center of the cap beam. The longitudinal seismic forces are balanced at the abutments by dedicated dissipative devices.

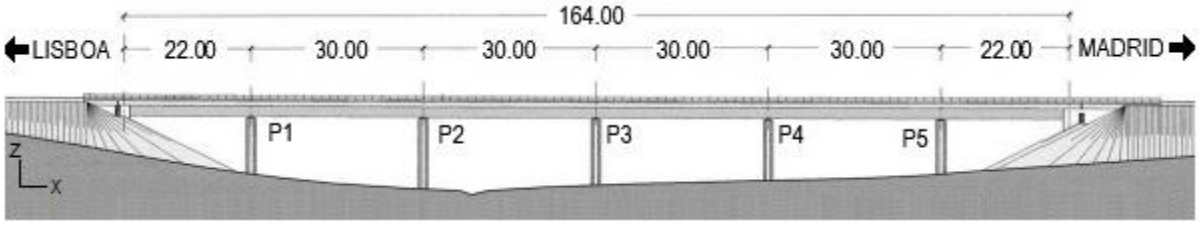


Figure 1: Analyzed Viaduct.

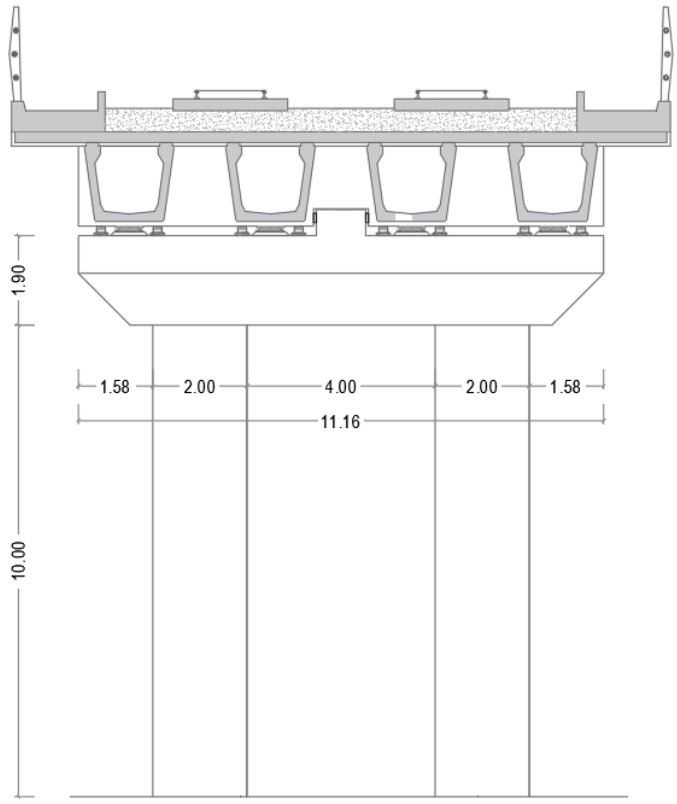


Figure 2: Two-column bents layout.

## 2.2 Substructure Design for Performance and Constructability

In the design, a force-based design approach was used, which meant that the columns were designed for maximum forces determined by a response spectrum analysis in SAP2000 [2]. Two design scenarios were performed to determine the seismic forces: an inelastic design spectrum with a behavior factor $q$=3.0, resulting in a maximum transversal seismic design force of 3.16MN in the governing alignment, and a behavior factor $q$=4.5, resulting in a maximum transversal seismic design force of 2.11MN in the governing alignment. The resulting reinforcement layout for both scenarios are presented in Figures 3 and 4, respectively.

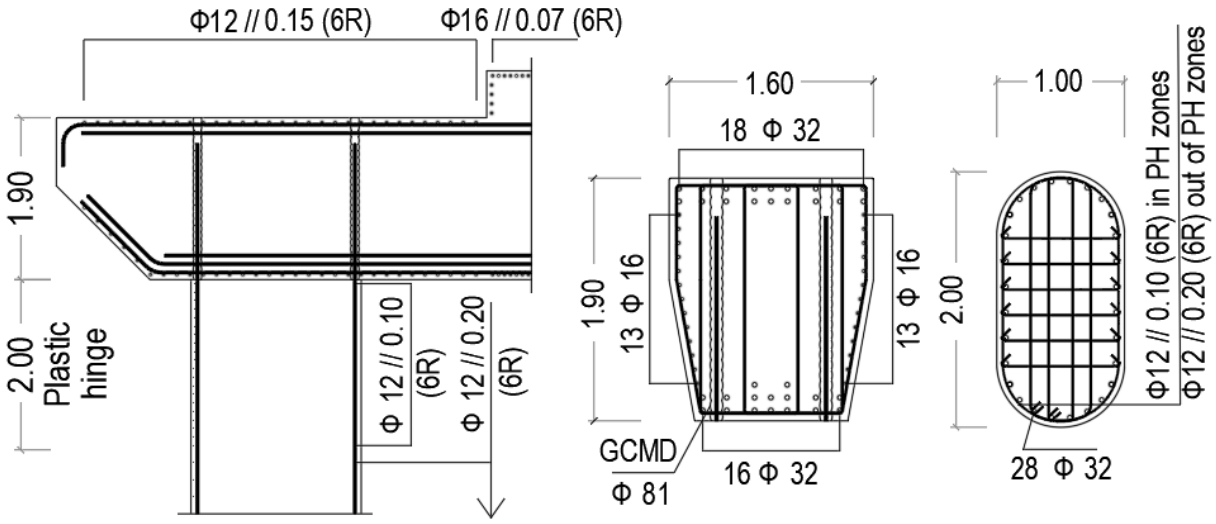


Figure 3: Column and cap-beam cross-sectional and reinforcement layout regarding scenario with q=3.0.

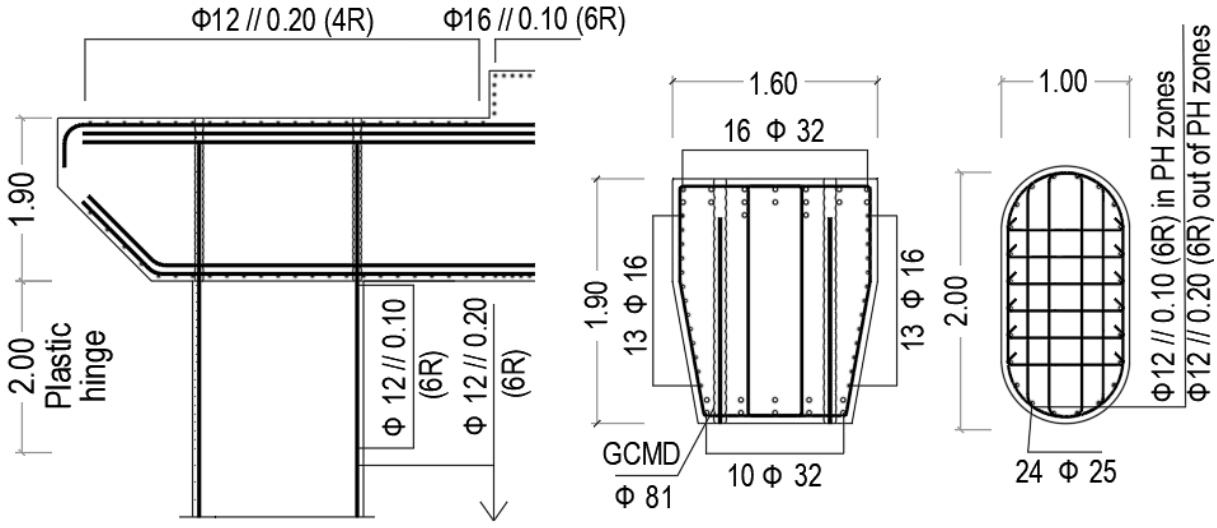


Figure 4: Column and cap-beam cross-sectional and reinforcement layout regarding scenario with q=4.5.

Concerned with constructive issues, a longitudinal reinforcement ratio of about 1.2% was considered, dictating the column geometry in the case with $q$=3.0. The geometry was maintained for the scenario with $q$=4.5. Also, the longitudinal reinforcement ratio ensures the viability of using corrugated ducts with diameters of 80mm to 100mm. The columns act as cantilevers in the longitudinal direction, and the corresponding second-order effects control the columns' minimum dimension. The minimum transversal stiffness of the railway bridge complying with the Eurocode 1 [3] requirements was also verified. The cap beam geometry was designed with weight constraints in mind, as well as the dimensions required to accommodate the final and temporary bearings during the assembly process, all while maintaining a reasonable reinforcement ratio and avoiding dense reinforcement layouts. The cap beam includes corrugated ducts distributed accordingly with the layout of the column vertical bars allowing a streamlined on-site assembly process. These ducts are posteriorly grouted for the anchorage of the vertical bars. As a fully precast solution is envisaged, special attention was paid to the reinforcement layout at the cap-columns joints. These are discontinuity regions, and the design was performed resorting to strut-and-tie models [4], as will be presented next.

## 3 STRUT-AND-TIE MODELS

Strut-and-tie models were developed [5] exploiting alternative load paths and load-bearing mechanisms, justifying the reinforcement layout to allow better constructability of the precast solution and ensuring the envisaged structural performance. Among these models, the showed in Figures 5 and 6, for design scenarios with $q$=3.0 and $q$=4.5, respectively, were the ones used for cap-beam design purposes. The reinforcement layout of Figures 3 and 4 was obtained by combining the results of models 1 and 2, for both design scenarios. For opening moments, model 1 allows the vertical bars from the column to be anchored in a straight manner, however, this requires additional vertical stirrups placed outside the column alignment to balance a fraction of the tensile force coming from the column, and additional longitudinal reinforcement in the bottom of the cap beam. Model 2 allows using horizontal reinforcement placed along the height of the cap beam to gradually reduce the vertical tensile force in the column bars. For closing moments, model 1 allows the vertical bars from the column to be anchored in a straight manner. Model 2 allows partial anchorage of the force in the vertical bars coming to the column due to the activation of the horizontal reinforcement crossing the joint.

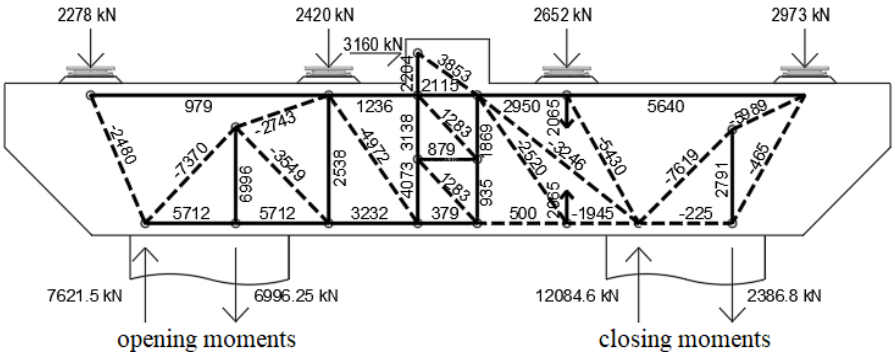


(a) model 1.

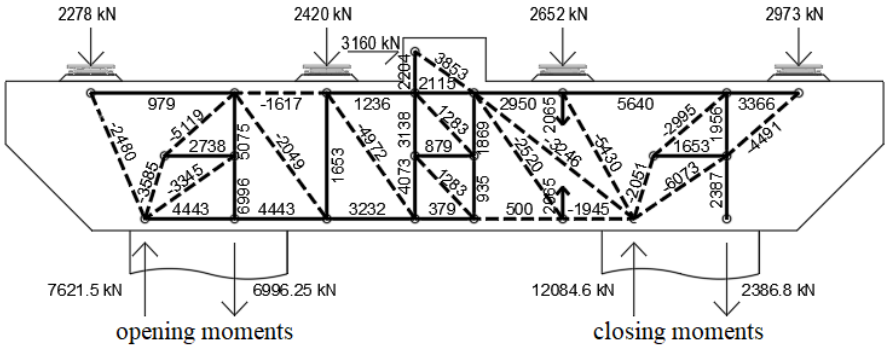


(b) model 2.

Figure 5: Strut-and-tie models corresponding to scenario with q=3.0.

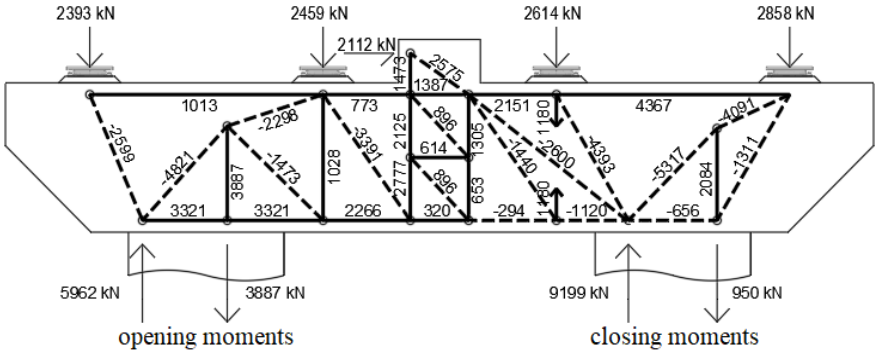


(a) model 1.

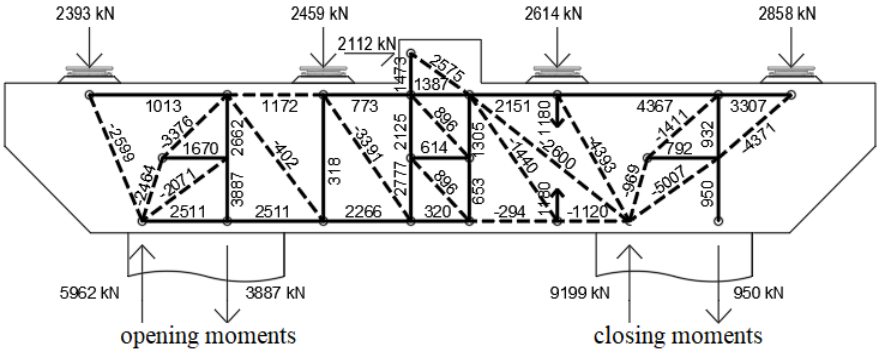


(b) model 2.

Figure 6: Strut-and-tie models corresponding to scenario with q=4.5.

It is noted that the vertical tie located at the left of the right column allows partial suspension of the shear forces coming from the leftmost part of the cap beam, with a fraction of the load being carried by direct strut action towards the column. This allows defining the same amount of transversal reinforcement in this region irrespective of the opening or closing rotation.

## 4 NONLINEAR NUMERICAL MODELING OF THE REDUCED SCALE MODEL

### 4.1 General

Three-dimensional finite element models were developed in the software DIANA 10.5 [6] to perform numerical simulations of 1/3.6 reduced scale prototypes, which were designed following Cauchy's similitude relationship. Also, an experimental campaign is being planned to evaluate the behavior of the column and cap-beam system under reversed horizontal loading. The objectives of these numerical simulations were to assess the redistribution of forces, mainly on the cap beam and joint zones to confirm the adequacy of the strut-and-tie models used in the design, to confirm the failure mode, quantify the ductility/energy dissipation capacity, and explore the results of both design scenarios. These prototypes such as the numerical models are hinged, at mid-height at the section of null flexural moment and can be seen in Figure 7. Noting that ZX is a symmetry plane, only half the structure is modelled using quadratic elements. The vertical forces in the four bearings were applied in a first step. Afterwards, the horizontal force at the corbel is increased monotonically until failure.

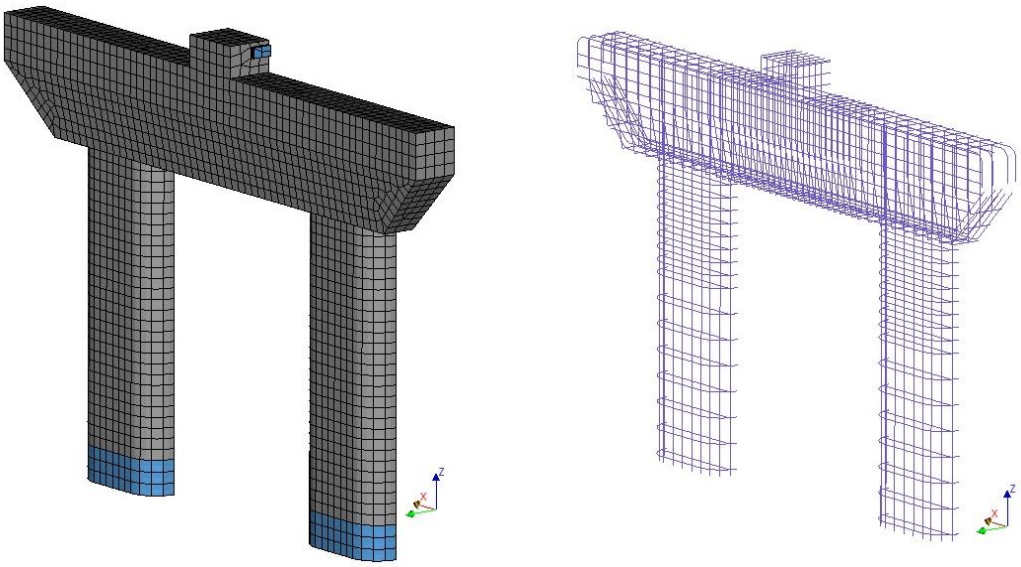

(a) finite element mesh. (b) reinforcements.

Figure 7: Nonlinear model concerning to $q$=3.0 scenario.

The principal material properties corresponding to the concrete strength class C40/45 and steel class A500 were adopted. All the reinforcements were explicitly included in the model. The transversal reinforcements are embedded, i.e., share the same displacement field of the concrete embedding elements. Otherwise, the longitudinal bars include bond-slip elements, allowing relative displacements between the reinforcements and concrete after cracking. The bond-slip curves were defined according to the fib Model Code 2010 [7], assuming the maximum bond shear stress $\tau_{b\,max}$ equal to 9.5 MN/m$^2$.

### 4.2 Model for Cracked Concrete

In the case under study, a total strain based rotating smeared crack model was used, which perform well in simulations of concrete structures with the concrete-reinforcement connection exhibiting a distributed cracking pattern. The rotating crack model considered has as its main assumption the reorientation of two axes of orthotropy according to the change in the crack orientation, always coinciding with the main deformation directions [8], leading to the advantage of having always shear stresses equal to zero, and thus avoiding the necessity of a law to describe the relationship between shear stresses and distortions.

### 4.3 Model for Compression Response

Concrete subjected to compressive stresses presents an inelastic behavior. The beginning of inelastic deformation occurs when the stress reaches approximately 30% of its compressive strength, after the peak of compressive strength, the stress decreases until compression failure occurs, when the maximum strain is reached [9]. To consider the nonlinear compression response in the modeling, a parabolic uniaxial compressive stress-strain curve [10] showed in Figure 8 (a) was selected, including a regularized post-peak branch defined by the compressive fracture energy, $G_C$ =60N/mm. The Hsieh-Ting-Chen failure envelope and multiaxial compressive stress states was adopted, as described in [11], allowing to restrict the transverse deformation of an element subject to axial compression, increasing the compression strength and the deformation capacity of the element, thus translating into a greater ductility capacity.

### 4.4 Model for Tensile Response

The crack band model was used to model tensile fracture. The strain softening curve is that proposed by Hordijk [12], showed in Figure 8 (b), defined by the tensile strength and by the fracture energy, $G_F$=0.09N/mm. The curve adopted aims to reproduce the decrease in tensile stresses in concrete as the width of the crack increases, since concrete is able to transmit residual stresses while the cracks are not fully formed. Also, the reduction of the Poisson effect due to cracking was considered in the model. When a crack is completely formed, the Poisson effect is null. Disregarding the reduction of the Poisson effect in which there is an important cracking process can cause a large error in estimating the structure deformations.

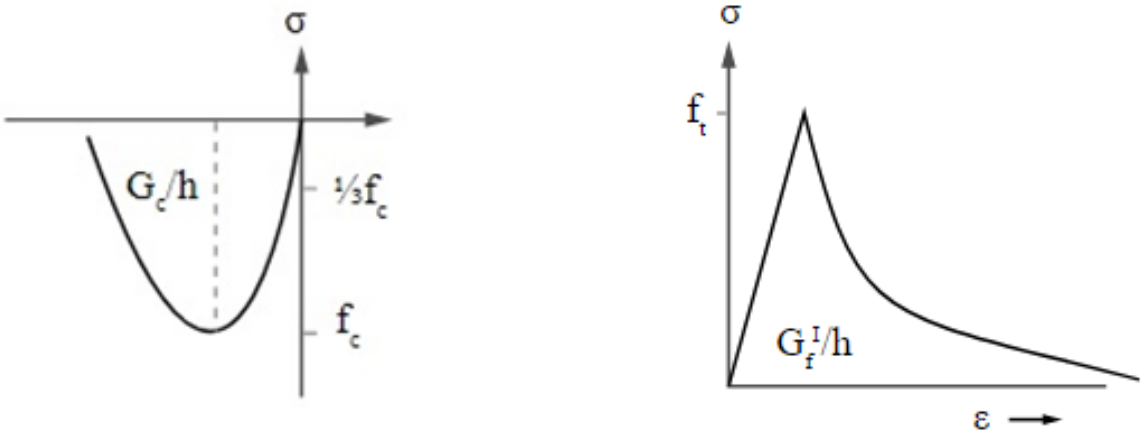


(a) Parabolic curve [10] (compression response). (b) Hordijk curve [12] (tensile response).

Figure 8: Constitutive curves.

### 4.5 Results

The lateral force vs. displacement curves is shown in Figure 9. Failure occurs with concrete crushing in the inner face of the right column, in both scenarios, after yielding of the flexural reinforcement in the columns. A yielding plateau is clearly visible in these curves. The straight dashed lines represent the lateral failure load $F_{pl}$ corresponding to the plastic mechanism involving the formation of the plastic hinges at the top of the columns. $F_{pl}$ was obtained considering the flexural strength of the columns determined by conventional sectional analysis methods considering the axial forces from the finite element model. The agreement with the maximum force achieved in the simulation is satisfactory.

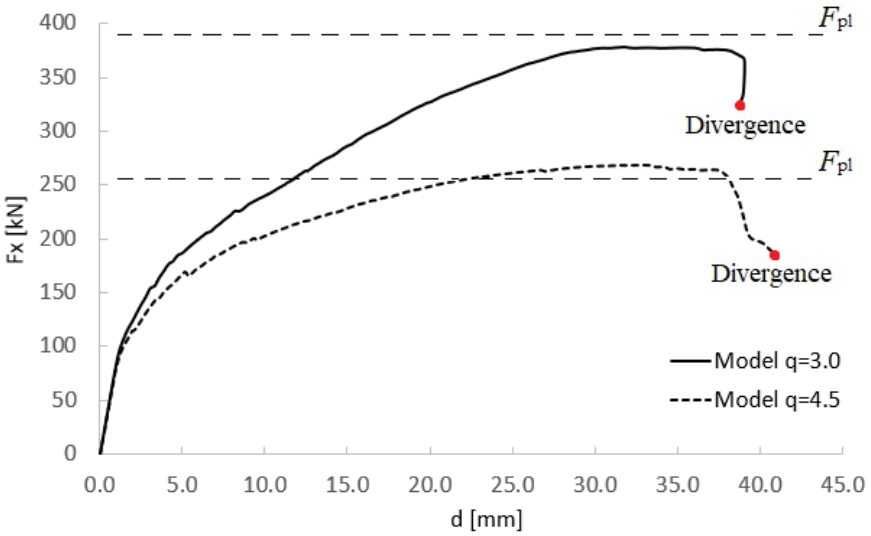


Figure 9: Force vs. displacement.

Figure 10 shows the color maps with the principal compressive stress values field and the cracking pattern right after the plastic mechanism has developed. These results are similar for both design scenarios, however, those presented in Figure 10 concern the design considering a behavior factor equal to $q$=4.5. In these results, a concentration of compression stresses in the inner face of the right column and a cracking distribution slightly accentuated in the left column can be observed.

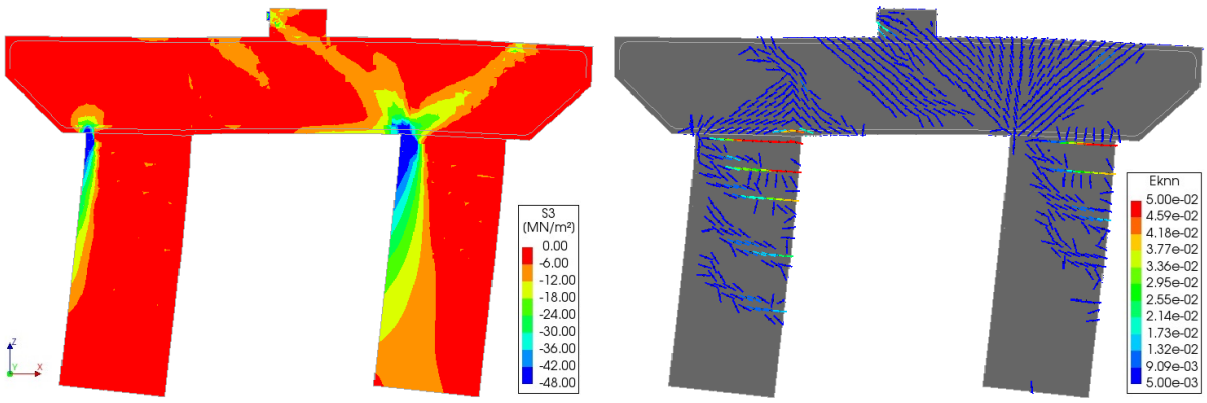


(a) principal compressive stress field. (b) cracking pattern.

Figure 10: Numerical results at the plastic mechanism stage concerning to $q$=4.5 scenario.

Figures 11 and 12 show the reinforcement stresses for both design scenarios right after the plastic mechanism has developed. At this stage, in both cases, most of the longitudinal reinforcement of the left column is yielding, as can be seen in Figure 11. Also, it is remarkable a greater contribution of the longitudinal reinforcement of the right column to the case with a higher behavior factor. Regarding the horizontal reinforcement, the cap beam in the first scenario is considerably most requested in comparison with the second scenario. In both cases, the column transverse reinforcements remain in the linear elastic range, as determined by the seismic design philosophy.

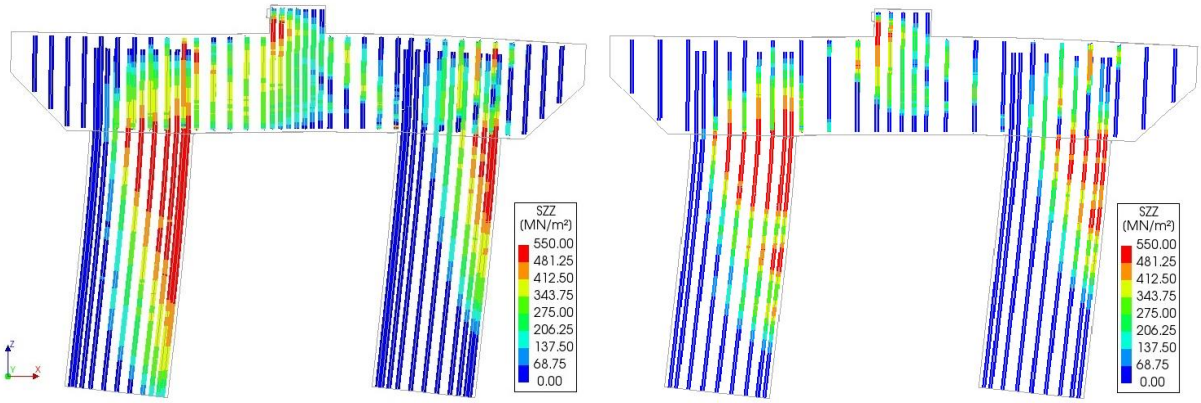


(a) scenario with $q$=3.0. (b) scenario with $q$=4.5.

Figure 11: Vertical bar stresses at the plastic mechanism stage.

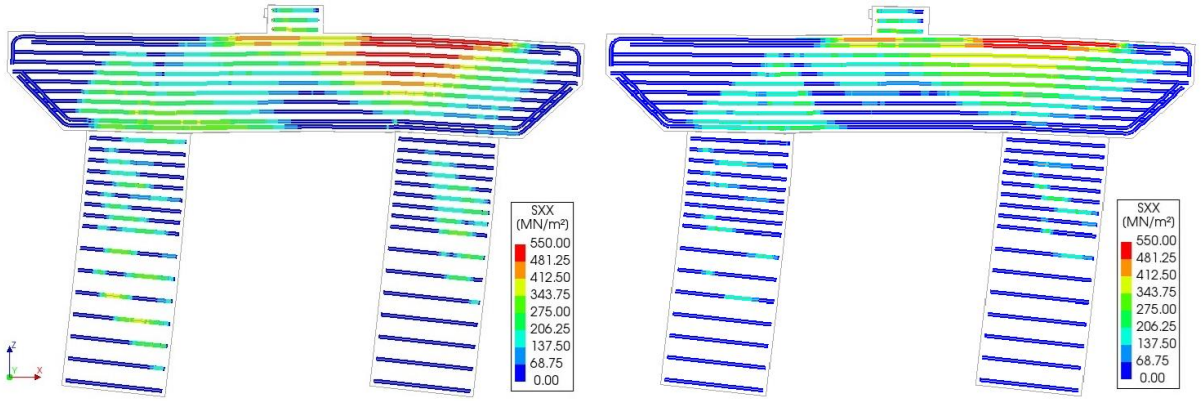


(a) scenario with $q$=3.0. (b) scenario with $q$=4.5.

Figure 12: Horizontal bar stresses at the plastic mechanism stage.

The reinforcements responsible for the transfer of forces between the column longitudinal bars and the cap beam, in the joint zone, ensure the formation of the plastic hinges in the columns, avoiding joint failure. This will be confirmed through experimental tests. However, to confirm the development of this phenomenon in the numerical model, a graph that shows the rotation evolution of the region where the plastic hinge was predicted with the increase in the flexural moment was made, which can be seen in Figure 13. From this analysis, it is visible that the plastic hinge develops on the left column, in both design cases, however, the energy dissipation mechanism on the right column has occurred only in the scenario with a behavior factor equal to q=4.5. In both cases, failure occurs due to concrete crushing, as evidenced in these graphs by the bending moment decreasing in the right column.

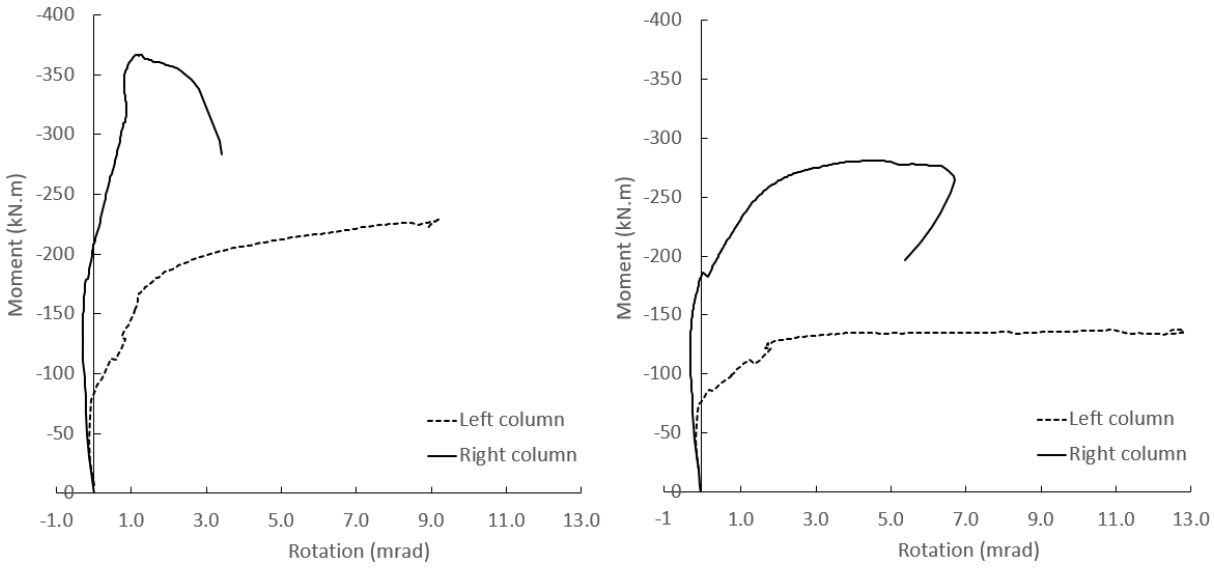


(a) scenario with $q$=3.0. (b) scenario with $q$=4.5.

Figure 13: Evolution of the plastic hinge rotation.

Figure 14 depicts the strut-and-tie models used on the design superposed to the principal compressive stress field taken from the nonlinear model. This analysis showed a good agreement of the strut-and-tie model configuration in comparison with the principal compressive stress field and allowed a good feasibility to the design.

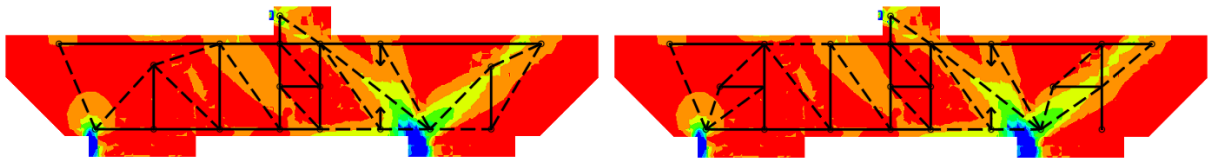

(a) model 1. (b) model 2.

Figure 14: Superposition between strut-and-tie models and principal compressive stress field.

## 5 CONCLUSIONS

- According to the results of the numerical investigation, satisfactory structural behavior could be evidenced as a result of the seismic design approach. In both cases, the structure achieved the yielding plateau at the force-displacement curve while the column longitudinal reinforcements were yielding, and the confinement reinforcements were at low levels of stress. Despite this, the structure failed due to concrete crushing in the inner face of the right column, preventing the plastic mechanism from progressing.
- Both design scenarios predicted the same displacement at failure, where the displacement capacity of the structure was limited by the same failure mechanism. Although this, the second scenario showed a post-yielding displacement larger than the first scenario.
- The second scenario showed greater activation of the right column longitudinal reinforcements, developing the plastic mechanism in both columns, unlike the first scenario, where the plastic hinge was developed only in the left column.
- Through the results from the non-linear numerical simulations, it was possible to assess the redistribution of forces on the cap beam and in the joint zones when subjected to hor-

izontal forces. Through this, the strut-and-tie models could be adjusted to reliably reproduce the mechanism of transfer forces that occur in that zone.

- The strut-and-tie models enabled a better reinforcement arrangement, avoiding constructive problems and maintaining reliable force paths, confirming the feasibility of using this approach to be applied in seismic design.
- This study is under development and all these conclusions will be confirmed through an experimental campaign that is being planned to assess the structural performance of the designed solution under reversed horizontal loading.

## ACKNOWLEDGEMENTS

This work is a result of project iPBRAIL - Innovative Precast Bridges for RAILways, with reference POCI-01-0247-FEDER-039894, co-funded by the European Regional Development Fund (ERDF), through the Operational Programme for Competitiveness and Internationalization (COMPETE 2020) and the Lisbon Regional Operational Programme (LISBOA 2020), under the PORTUGAL 2020 Partnership Agreement. The authors also acknowledge the financial support by: Base (UIDB/04708/2020) and Programmatic (UIDP/04708/2020) funding of CONSTRUCT financed by national funds through the FCT/MCTES (PIDDAC). This work was also developed within the scope of the project proMetheus – Research Unit on Materials, Energy and Environment for Sustainability, FCT Ref. UID/05975/2020, financed by national funds through the FCT/MCTES.


## REFERENCES

[1] Lou Ralls, M. *Accelerated Bridge Construction*. ASPIRE, Spring, 2007.

[2] CSI. *SAP2000_v22.1.0 – Finite element program for modelling, analysis, and design of any type of structure*. Help documentation of the program, https://www.csiportugal.com/, 2020.

[3] (CEN) European committee for standardization. *Eurocode 1 - Actions on structures. Part 2: Traffic loads on bridges*. Brussels, 2017.

[4] J. Schlaich, K. Schaefer, and M. Jennewein. *Toward a consistent design of structural concrete*. PCI Journal, vol. 32, no. 3, 1987.

[5] Carvalho, L., Pimentel, M., Arêde, A., Vila Pouca, N., Delgado, P., Pinto, J.R. *Design of pre-cast two-column bents using strut-and-tie models and nonlinear finite element analysis.* fib Symposium – Structural Performance and Design. Istanbul, Turkey, 2023.

[6] "DIANA," Release 10.4, TNO DIANA BV, Delft, The Netherlands, 2012.

[7] International Federation for Structural Concrete (fib). *Fib Model Code for Concrete Structures 2010*. Ernst & Sohn, Switzerland, 2013.

[8] Rots, J., Blaauwendraad, J. *Crack models for concrete: Discrete or smeared? Fixed, multi-directional or rotating?*. Delft University of Technology, Faculty of Civil Engineering. 1989.

[9] Deaton, J. *Nonlinear finite element analysis of reinforced concrete exterior beam-column joints with nonseismic detailing*. School of Civil and Environmental Engineering. Georgia Institute of Technology, 2013.

[10] Feenstra, P. H. *Computational Aspects of Biaxial Stress in Plain and Reinforced Concrete*. PhD thesis, Delft University of Technology, 1993.

[11] Selby, R. G., and Vecchio, F. J. *Three-dimensional Constitutive Relations for Reinforced Concrete*. Tech. Rep. 93-02, Univ. Toronto, dept. Civil Eng., Toronto, Canada, 1993.

[12] Hordijk, D. *Local approach to fatigue of concrete*. Doctoral Thesis Universiteit Delft, 1991.